

A Distributed Secondary Control for Autonomous AC Microgrid Based on Photovoltaic and Energy Storage Systems



Sidlawendé V. M. Ouoba, Azeddine Houari, and Mohamed Machmoum

Abstract In this paper, a distributed control is proposed for Distributed Energy Storage Systems (DESSs) and Renewable Energy Sources (RESs) power management in islanded Microgrid (MG). The power management strategy is designed to maintain generation/consumption balance, to ensure State of Charge (SoC) balancing of the DESSs and MG frequency/voltage (f & V) regulation. A fully distributed control without leader-follower strategy is used to manage the power flow between renewable generators, energy storage and consumption (critical and non-critical loads), to balance the SoC of the DESSs and to restore the frequency and voltage to their nominal value only thanks to low bandwidth communication. The strategy framework of the power management set the islanded MG in 04 operations modes (normal mode, PV active power curtailment mode and load shedding and reconnection mode) in order to provide a high quality and reliable power source in the islanded MG. A MATLAB/Simulink simulation is performed with a system of two Batteries Energy Storage Systems (BESSs), three loads (a critical/variable load and two non-critical/constant loads) and photovoltaic (PV) generator, in order to verify the effectiveness and the resilience of the proposed power management method in several operation modes.

1 Introduction

Distributed Energy Storage Systems (DESSs) are widely used in MG operation in order to assist RESs which have intermittent nature [1]. The mix of DESSs with RESs improves significantly the MG reliability, flexibility and power quality [2]. ESSs are vital in islanded MG in order to compensate the short-term mismatch power between RESs and loads [3].

S. V. M. Ouoba (✉) · A. Houari · M. Machmoum
IREENA – Nantes Université, Saint Nazaire, France
e-mail: sidlawende.ouoba@etu.univ-nantes.fr; Azeddine.Houari@univ-nantes.fr;
Mohamed.Machmoum@univ-nantes.fr

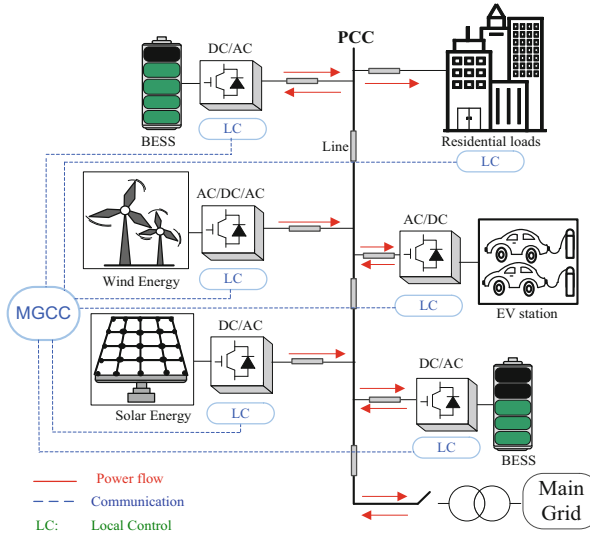


Fig. 1 Typical configuration for an AC microgrid system with distributed storage systems

Coordinated control is indispensable in this case to achieve power management between RESs, energy storage and loads in order to enhance the MG reliability, flexibility and power quality. This coordinated control is used to balance and maintain the SoC of DESSs in a certain range (20–90%), to maintain generation/consumption balance and to regulate frequency/voltage.

DESSs and RESs power management strategy has many benefits. First, DESSs SoC balancing extends their lifetime by avoiding deep discharge and surcharge and reducing the BESSs charge/discharge cycles that caused premature ageing. Second generation/consumption balance allows to supply power to critical loads longer especially when a power mismatch between distributed generators (RESs and DESSs) and loads is observed.

Coordinated control can be achieved by using a centralized (Fig. 1) or a distributed architecture controller. A centralized architecture uses a MGCC (Microgrid Central Controller) to achieve the power management between DESSs and RESs by exchanging data with all DGs while a distributed architecture controller only exchanges information between DGs through a sparse communication network. In a distributed architecture, each agent receives information from its neighbors. Unlike centralized control architecture which has a unique point of failure (MGCC default), the distributed architecture allows the continuity of system control when a communication failure happens and improves the system reliability and expandability.

Many methods have been proposed to ensure coordinated control between RESs and DESSs. Conventionally, centralized control is used for the coordinated operation of DESSs, RESs units and loads. Reference [4] used a centralized control architecture for the coordinated operation, where SoC equalization is achieved

between DESSs with different capacities by adjusting the frequency droop gain value. Nevertheless, centralized architecture control possesses the single point of failure that may cause loss of the coordination of the Microgrid and modifying the droop gain may bring stability issues. In [5], a distributed control based on leader-follower is implemented to ensure power management and DESSs SoC balancing. In order to maintain generation/consumption balance, load shedding and PV curtailment are introduced. However, since this strategy was used in DC MG, frequency regulation is not implemented.

In this paper, a fully distributed control is used for coordinated operation of DESSs, RESs units and loads to ensure a reliable and stable operation of an AC islanded MG based PV-DESSs. The power management strategy achieves PV active power curtailment to prevent DESSs surcharge; loads shedding to avoid the storage systems from deep discharge and DESSs SoC balancing in order to reduce the storage systems charge/discharge cycles that caused premature ageing and to avoid uneven degradation. The Adaptive Frequency Droop based on Virtual Power (AFDVP) method is used for SoC synchronization. This method introduces a virtual power in the $P-\omega$ equation of the droop that is determined with a simple PI controller. In addition, frequency and voltage regulation is implemented in a distributed control architecture. In this proposal, active power curtailment, loads shedding, SoC balancing as well as frequency and voltage restoration are achieved in a fully distributed architecture controller therefore the proposed method is robust against communication failure. Information in this architecture is exchanged through a sparse communication network. The main contributions of this proposal are as follows:

1. The proposed coordinated control is fully distributed without a leader-follower strategy and is resilient to communication failure.
2. Frequency regulation is implemented in coordinated control with SoC balancing to maintain the frequency of the DGs at the nominal frequency of the MG.
3. Proposed algorithms for load shedding and PV curtailment are simple to implement.

The rest of the paper is organized as follows: In Sect. 2, the studied system is presented. AFDVP and voltage/frequency regulation method implementation in a distributed control architecture are investigated in Sect. 3. In Sect. 4, coordinated control algorithm for PV-DESSs based islanded MG is explained. Simulation results are presented in Sects. 5 and 6 concludes this paper.

2 Studied System

The general synoptic scheme of the studied system is presented in Fig. 2. This System represents an islanded AC Microgrid with two batteries and photovoltaic source supplying three loads (two non-critical and constant loads and one critical and variable load) connected the AC bus. All Distributed Generators (DESSs and

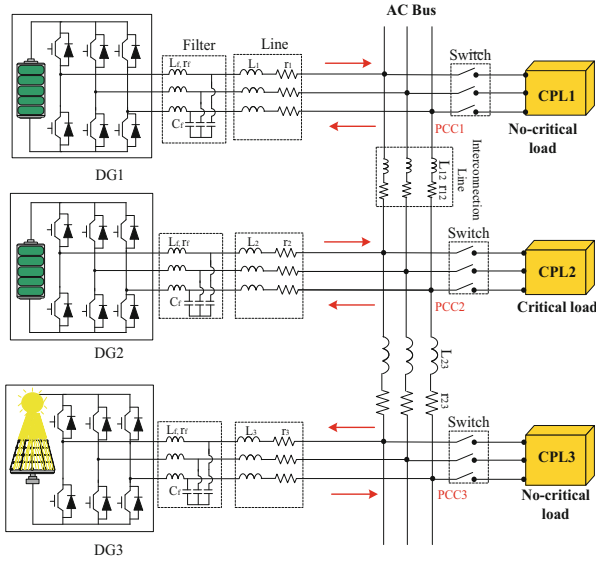


Fig. 2 Studied system

PV) are relied to the AC bus through inverters. In the next section, the AFDVP strategy is presented, to ensure DESSs SoC synchronization.

3 SoC Balancing and Voltage/Frequency Regulation in a Fully Distributed Architecture Controller

Distributed control is recently widely used in MG especially for secondary control. It is a promising approach to enhance islanded MG reliability, stability and performance [6]. Many works have been already proposed to ensure distributed secondary control [7–9]. Distributed control has many advantages such as reduction of the communication infrastructure cost, reduction of computational burden, is more reliable and adapted for large and complex MG compare to the centralized control.

In this section, a fully distributed control architecture is used for DESSs SoC synchronization and voltage/frequency restoration.

3.1 Graph Theory and Distributed Control Based on Consensus

The communication network can be expressed by a graph $G = (V, E)$, with $V = \{v_1, v_2, \dots, v_N\}$, the set of N nodes or N agents and $E \subseteq V \times V$, the set of

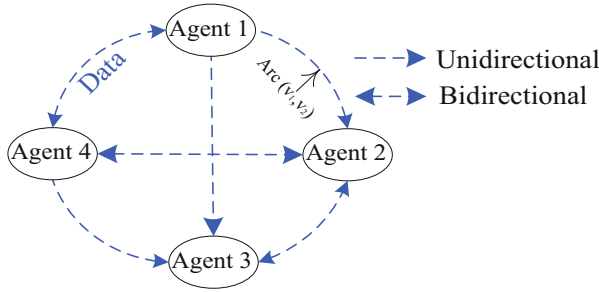


Fig. 3 Graph with four agents

edges or arcs. Elements of E are denoted as (v_i, v_j) and represent the arcs from node v_i to node v_j and are represented with arrows at unique or double direction depending on the information flow between the two agents (unidirectional or bidirectional) as represented in Fig. 3.

Each edge (v_i, v_j) is associated with a weight $a_{ij} > 0$ if v_i receives information from v_j else $a_{ij} = 0$. The adjacency matrix is defined as: $A = [a_{ij}]$ and the graph Laplacian matrix as $L = D - A$. D the diagonal matrix is defined as: $D = \text{diag} \{d_i\}$ and $d_i = \sum_{j=1}^N a_{ij}$.

In order to bring all the agents (x_j) to converge to the same value (x_0), the distributed control-based consensus protocol is defined as:

$$\mu_i = \sum_{j=1}^N a_{ij} (x_j - x_i) + b_i (x_i - x_0) \tag{1}$$

where $b_i > 0$ if the agent v_i has the information about the consensus value, otherwise $b_i = 0$.

With this protocol, the global dynamics of the consensus control protocol can be defined as:

$$\dot{X} = K (-LX + B (X_0 - X)) \tag{2}$$

where $X = [x_1, \dots, x_N]'$; $X_0 = [x_{01}, \dots, x_{0N}]'$; $B = \text{diag} \{b_i\}$, the diagonal pinning matrix; $L = D - A$, the Laplacian matrix and K , the consensus gain.

For the studied system defined in Fig. 2, the adjacency matrix A and Laplacian Matrix L can be defined respectively as:

$$A = \begin{pmatrix} 0 & 1 & 1 \\ 1 & 0 & 1 \\ 1 & 1 & 0 \end{pmatrix}, L = \begin{pmatrix} 2 & -1 & -1 \\ -1 & 2 & -1 \\ -1 & -1 & 2 \end{pmatrix}; B = \begin{pmatrix} 1 & 0 & 0 \\ 0 & 1 & 0 \\ 0 & 0 & 1 \end{pmatrix}$$

3.2 DESSs SoC Balancing and Voltage/Frequency Regulation

In this section, a distributed control-based consensus control is used for frequency/voltage regulation and the AFDVP method in [10] is used for DESSs SoCs synchronization. Equations for the distributed control-based consensus to calculate f & V compensators are designed as follows:

$$\dot{X}_v = K_v (-L\bar{V} + B(\bar{V}_n - \bar{V})) \quad (3)$$

$$\dot{X}_\omega = K_\omega (-LW + B(W_n - W)) \quad (4)$$

with $X_v = [x_{1v}, x_{2v}, x_{3v}]'$; $\bar{V} = [V_1, V_2, V_3]'$; $\bar{V}_n = [V_n, V_n, V_n]'$; $X_\omega = [x_{1\omega}, x_{2\omega}, x_{3\omega}]'$; $W = [\omega_1, \omega_2, \omega_3]'$; $W_n = [\omega_n, \omega_n, \omega_n]'$; where K_v , K_ω : voltage and frequency consensus control gain respectively; L : Laplacian matrix; B : diagonal pinning Matrix and x_{iv} , $x_{i\omega}$: voltage and frequency compensator of the *DESS*_{*i*} respectively.

The global dynamic equations for voltage/frequency restoration and SoC equalization are as follows:

$$V_i = V_n - n_i (Q_i - Q_{in}) + x_{iv} \quad (5)$$

$$\omega_i = \omega_n - m_i (P_i - P_{in} + P_{iSoC}) + x_{i\omega} \quad (6)$$

$$P_{iSoC} = K_{pSoC} \Delta SoC_i + K_{iSoC} \int \Delta SoC_i dt \quad (7)$$

with P_{iSoC} : the virtual power for SoC balancing; K_{pSoC} : the PI proportional coefficient; K_{iSoC} : the PI integrator coefficient.

In the next section, proposed algorithms for PV active power reduction and load shedding are presented.

4 Proposed Fully Distributed Control for RESs and DESSs Coordinated Operation

This section introduces a fully distributed control for coordinated operation of DESSs, RESs units and loads to ensure a reliable and stable operation of an AC Microgrid. The optimized power management strategy should ensure PV active power curtailment (during daytime when PV generation is maximum and DESSs are almost fully charged) to prevent DESSs surcharge and loads shedding in order to avoid deep surcharge during night (no PV generation). This proposal also includes a

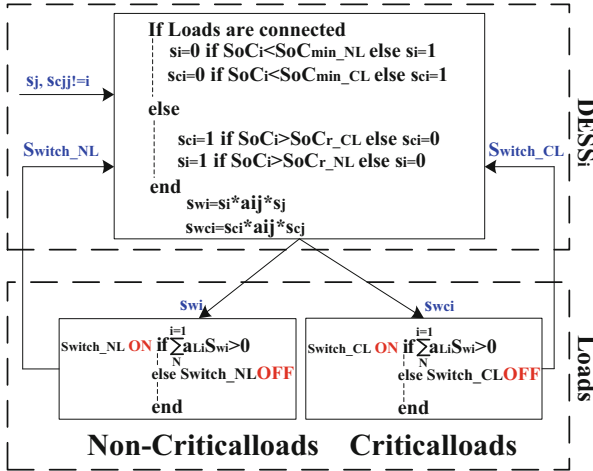


Fig. 4 Algorithm for load shedding (mode 2) and reconnection (mode 3)

management for critical loads (CL) and non-critical loads (NL). Non-critical loads should be disconnected first when DESSs state of charge is below the minimum state of charge (SoC_{min}). Then, critical load should be disconnected to the MG only when DESSs SoCs reach a critical value (SoC_{minc}). Loads are reconnected only when DESSs SoCs reach a value of safe reconnection (SoC_r for non-critical loads and SoC_{rc} for critical loads).

The proposed method to ensure load shedding, uses signals based on DESSs SoCs (s_i and s_{ci}) which are exchanged between the DESSs. Each DESS sends a signal to the loads according to its local information, information received from its neighbors and the loads (critical and non-critical). Loads are disconnected if one of the DESSs SoCs reach a minimum value (SoC_{min_NL} , SoC_{min_CL}) and reconnected if all DESSs SoCs reach a safe range for reconnection (SoC_{r_NL} or SoC_{r_CL}). The proposed strategy algorithm for load shedding is reported in Fig. 4.

PV curtailment is ensured thanks to signals (k_i) that are exchanged between DESSs and PV. When DESSs states of charge reach the maximum value (SoC_{max}), PV active power (P_{pv}) is reduced according to the curtailment coefficient (k_{pv}) calculated using the loads total active power (P_{Loads}) sends by the loads to the PV unit local controller. k_{pv} is determined in order to maintain the SoC of DESSs at SoC_{max} ($SoC_i = SoC_{max}$, $P_{pv} = P_{Loads}$, $P_{DESSs} = 0$). Proposed algorithm for PV curtailment is represented in Fig. 5. All operational mode of the MG is reported in Fig. 6.

The global communication network of the whole MG is represented in Fig. 7.

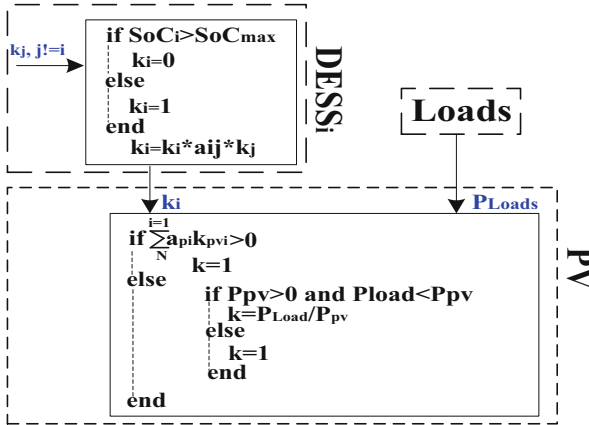


Fig. 5 Algorithm for PV curtailment (mode 4)

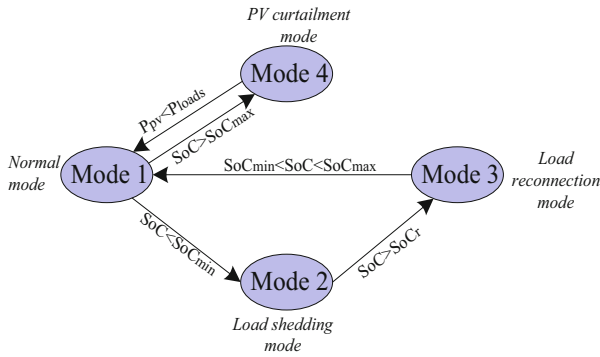
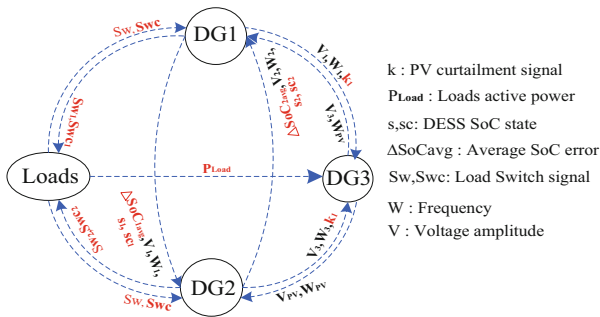


Fig. 6 Operations modes of the MG



- k : PV curtailment signal
- P_{Load} : Loads active power
- s,sc: DESS SoC state
- ΔSoC_{avg} : Average SoC error
- Sw, Swc: Load Switch signal
- W : Frequency
- V : Voltage amplitude

Fig. 7 Global communication network system

5 Simulation Results

To investigate the proposed coordinated strategy, a MATLAB/Simulink simulation is performed on the studied system reported in Fig. 2 for 1 day of operation with a typical PV active power curve and residential load consumption. Systems parameters are reported in Table 1. Two tests are realized: First test is realized to validate the effectiveness of the proposed power management strategy without communication failure. Second test is performed to show the resilience and robustness of the proposed coordinated control in the event of a communication network failure. For both tests, the DESS 1 and 2 SoCs are set initially to 87% and 80% respectively and all three loads are also connected to the MG.

5.1 Test 1: Typical Day Operation

First test is devoted to validate the effectiveness of the proposed method. The simulation results are reported in Fig. 8. PV active power and residential load active power profile for the day are represented in Fig. 8a. Loads switches signals and PV curtailment coefficient are reported in Fig. 8b. The SoC of the DESSs are presented in Fig. 8d and DGs active power in Fig. 8c.

At 0 h to 4 h, $P_{PV} = 0$ only the batteries ensure power supply to the loads. However, at 6 h 51 min, even if PV started to supply power, the CPL 1 and 3 are

Table 1 System parameters

Item	Symbol	Value
<i>MG parameters</i>		
Impedance line DG1	r_1, L_1	0.1 Ω , 1 mH
Impedance line DG2	r_2, L_2	0.2 Ω , 2 mH
Impedance line DG3	r_3, L_3	0.3 Ω , 2.5 mH
Impedance line DG1-DG2	r_{12}, L_{12}	0.1 Ω , 1 mH
Impedance line DG2-DG3	r_{23}, L_{23}	0.1 Ω , 2 mH
Max active power DG1	P_{1n}	2800 W
Max active power DG2	P_{2n}	2900 W
Max active power DG3	P_{3n}	4000 W
CPL 1 active power	P_{CPL1}	350 W
CPL 2 active power	P_{CPL2}	1000–1500 W
CPL 3 active power	P_{CPL3}	300 W
MG frequency/voltage	f_n/V_n	50 Hz/230 V
<i>Control parameters</i>		
Max f & V deviation	$\Delta f/\Delta V$	0.5 Hz/5 V
PI for SoC balancing	$K_{pSoC}; K_{iSoC}$	800; 2
Frequency consensus gain	K_ω	20
Voltage consensus gain	K_V	10

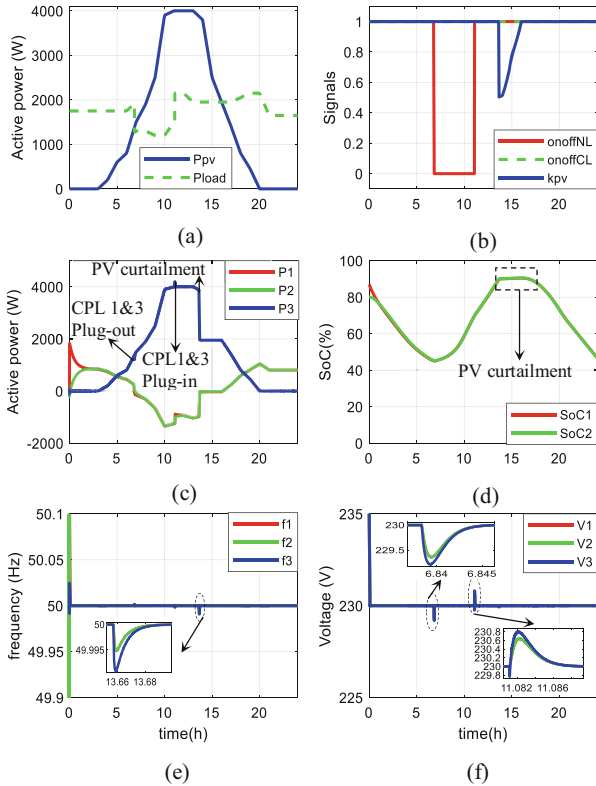


Fig. 8 Typical day operation of the islanded MG: (a) Load and PV power profile (b) Control signals (c) DGs active power (d) SoC of DGs (e) Frequency of DGs (f) Voltage of DGs

plugged-out when $SoC_i < SoC_{min_NL}$ (45%). At this moment, batteries started to recharge since $P_{PV} < P_{Loads}$. Batteries are recharged to SoC_{r_NL} (70%) then the CLP 1 and 3 are reconnected to the grid at 11 h 04 min. PV curtailment mode is activated at 13 h 37 min as soon as the SoC of BESSs reaches SoC_{max} (90%) until $P_{PV} < P_{Loads}$ at 16 h. The MG operates in normal mode, photovoltaic and batteries ensure the power supply of the loads.

It is also worth mentioning that voltage (Fig. 8f) and frequency (Fig. 8e) are maintained to their nominal value during the MG operation despite load shedding and variation. Slight peaks of DESSs voltage and frequency appear during load variations. However, these peaks are negligible compare to the limited variations range. The SoCs of all BESSs are also well synchronized during the operating day.

5.2 Test 2: Communication Network Failure

Second test is dedicated to the robustness of the proposed method against communication failure. In order to see the impact of communication failure on the proposed coordinated method, a communication link failure between the agent 1 and 3 is simulated as reported in Fig. 9. Information exchange between the DG1 and the DG3 is no longer possible ($a_{13} = 0$ and $a_{31} = 0$). PV active power and the residential load active power profile for 1 day are the same as those used in the first test and are shown in Fig. 10a. The simulation results are illustrated in Fig. 10. Loads switches signals and PV curtailment coefficient are reported in Fig. 10b. The SoC of the DESSs are presented in Fig. 10d and DGs active power in Fig. 10c.

Results show that despite the loss of communication between the two agents (1 and 3), the coordinated control (load shedding and PV curtailment) continues to work perfectly. Indeed, even if the information on the state of the DG1 is not directly received by the DG3, this information is transmitted to the DG2 which will then transmit it to the DG3. The convergence speed of the SoC balancing becomes slower but works properly (Fig. 10d). Frequency and voltage of the DESSs remained to their nominal (Fig. 10e, f) value during all the MG operation therefore their regulation control is also resilient to the loss of the communication link.

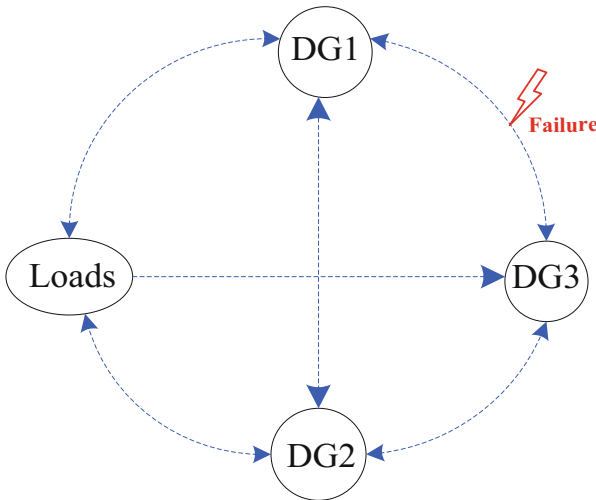


Fig. 9 Communication failure event between DG1 and DG3

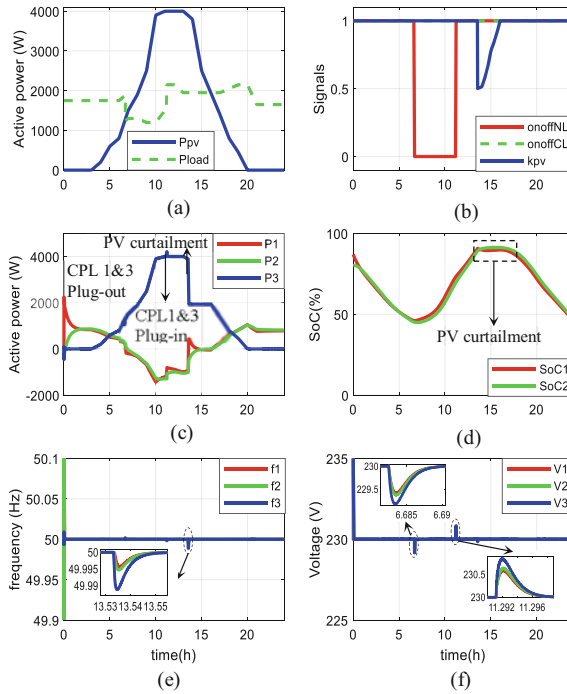


Fig. 10 Test with communication failure between DG1 and DG3: (a) Load and PV power profile (b) Control signals (c) DGs active power (d) SoC of DGs (e) Frequency of DGs (f) Voltage of DGs

6 Conclusions

In this paper a fully distributed control has been proposed to ensure coordinated operation in an autonomous MG based PV-DESSs. The design objective is to achieve power management by ensuring SoC balancing of the DESSs, PV curtailment, load shedding and frequency/voltage regulation. The main contributions are the use of a fully distributed resilient control for the coordinated control, the implementation of frequency regulation and algorithms for PV curtailment and load shedding.

The proposed coordination control is validated through a MATLAB/Simulink simulation for a system of two BESSs and a PV panel linked to an AC bus supplying variable and constant loads. Simulation results show the effectiveness and the resilience of the proposed power management strategy during a typical day of operation and show that all four operations modes of the MG work perfectly even in the event of failure in the communication network.

References

1. G. Shi, H. Han, Y. Sun, Z. Liu, M. Zheng, et X. Hou, « A Decentralized SOC Balancing Method for Cascaded-Type Energy Storage Systems », *IEEE Transactions on Industrial Electronics*, vol. 68, n° 3, p. 2321–2333, mars 2021, <https://doi.org/10.1109/TIE.2020.2973889>.
2. L. Chang, W. Zhang, S. Xu, et K. Spence, « Review on distributed energy storage systems for utility applications », *CPSS Transactions on Power Electronics and Applications*, vol. 2, n° 4, p. 267–276, déc. 2017, <https://doi.org/10.24295/CPSSPEA.2017.00025>.
3. D. Wu, F. Tang, T. Dragicevic, J. C. Vasquez, et J. M. Guerrero, « A Control Architecture to Coordinate Renewable Energy Sources and Energy Storage Systems in Islanded Microgrids », *IEEE Transactions on Smart Grid*, vol. 6, n° 3, Art. n° 3, mai 2015, <https://doi.org/10.1109/TSG.2014.2377018>.
4. N. L. Díaz, A. C. Luna, J. C. Vasquez, et J. M. Guerrero, « Centralized Control Architecture for Coordination of Distributed Renewable Generation and Energy Storage in Islanded AC Microgrids », *IEEE Transactions on Power Electronics*, vol. 32, n° 7, p. 5202–5213, juill. 2017, <https://doi.org/10.1109/TPEL.2016.2606653>.
5. M. S. Golsorkhi, Q. Shafiee, D. D.-C. Lu, et J. M. Guerrero, « A Distributed Control Framework for Integrated Photovoltaic-Battery-Based Islanded Microgrids », *IEEE Transactions on Smart Grid*, vol. 8, n° 6, p. 2837–2848, nov. 2017, <https://doi.org/10.1109/TSG.2016.2593030>.
6. Y. Khayat *et al.*, « On the Secondary Control Architectures of AC Microgrids: An Overview », *IEEE Transactions on Power Electronics*, vol. 35, n° 6, p. 6482–6500, juin 2020, <https://doi.org/10.1109/TPEL.2019.2951694>.
7. J. Hu et P. Bhowmick, « A consensus-based robust secondary voltage and frequency control scheme for islanded microgrids », *International Journal of Electrical Power & Energy Systems*, vol. 116, p. 105575, mars 2020, <https://doi.org/10.1016/j.ijepes.2019.105575>.
8. H. Ali, A. Hussain, V.-H. Bui, et H.-M. Kim, « Consensus Algorithm-Based Distributed Operation of Microgrids During Grid-Connected and Islanded Modes », *IEEE Access*, vol. 8, p. 78151–78165, 2020, <https://doi.org/10.1109/ACCESS.2020.2989457>.
9. M. A. Shahab, B. Mozafari, S. Soleymani, N. M. Dehkordi, H. M. Shourkaei, et J. M. Guerrero, « Distributed Consensus-Based Fault Tolerant Control of Islanded Microgrids », *IEEE Transactions on Smart Grid*, vol. 11, n° 1, Art. n° 1, janv. 2020, <https://doi.org/10.1109/TSG.2019.2916727>.
10. S. Ouoba, A. Houari, et M. Machmoum, « Robust SoC Balancing Method for Distributed Storage based Islanded Microgrids », in *IECON 2021 – 47th Annual Conference of the IEEE Industrial Electronics Society*, oct. 2021, p. 1–6. <https://doi.org/10.1109/IECON48115.2021.9589165>.